

# Adjusted ADM systems and their expected stability properties

Hisa-aki Shinkai\* and Gen Yoneda†

\* *Computational Science Division,  
Institute of Physical & Chemical Research (RIKEN),  
Hirosawa 2-1, Wako, Saitama, 351-0198 Japan*

† *Department of Mathematical Sciences,  
Waseda University, Shinjuku, Tokyo, 169-8555, Japan*  
(Dated: September 30, 2001 gr-qc/0110008)

In order to perform a long-term stable and accurate numerical evolution of the Einstein equations, we here study the propagation equations of the constraints based on the Arnowitt-Deser-Misner formulation. Our purpose is to construct “an asymptotically constrained system” by adjusting constraint terms in the dynamical equations. We provide useful expressions for analyzing constraint propagation in general spacetime first, then apply it to the Schwarzschild spacetime. We search when and where the negative real or non-zero imaginary eigenvalues of the homogenized constraint propagation matrix appear, and how they depend on the choice of coordinate system and adjustments. Our analysis includes the proposal of Detweiler (1987), which is still the best one in total but has a growing mode of the error near the horizon. Some examples are of snapshots of maximally sliced Schwarzschild black hole. The predictions here may help the community further improvements.

## I. INTRODUCTION

The current important issue in numerical relativity is to determine which formulation of the Einstein equations provides us with stable and accurate simulations. Spending decades, we begin noticing that the standard Arnowitt-Deser-Misner (ADM) formulation [1, 2] (especially we say the “standard ADM” for the version introduced by York [2]) is not the best formulation to perform numerical simulations such as black hole or neutron star binary coalescences.

At this moment, there may be three major directions to obtain longer time evolutions. The first one is to use a modification of ADM system that was developed by Shibata and Nakamura [3] (and later remodified by Baumgarte and Shapiro [4]). This is a combination of the introduction of the new variables, conformal decompositions, rescaling the conformal factor, and replacement of terms in evolution equation using momentum constraints. Although there are many studies to show why this re-formulation is better than the standard ADM, but as far as we know, there is no definite conclusion yet. One observation [5] pointed out that to replace terms using momentum constraints changes the stability properties apparently.

The second direction is to re-formulate the Einstein equations in a first-order hyperbolic form [6]. This is motivated from the expectation that the symmetric hyperbolic system has well-posed properties in its Cauchy treatment in many systems and also that the boundary treatment can be improved if we know the characteristic speed of the system. We note that, in the way of constructing hyperbolic systems, the essential procedures are to adjust equations using constraints and to introduce new variables, normally the spatially derivatived metric. Several groups reported that the hyperbolic formulation actually has advantages than the direct use of ADM formulation [7, 8, 9, 10]. However it is also reported that there is no drastic changes in the evolution properties *between* hyperbolic systems (weakly/strongly and symmetric hyperbolicity) by systematic numerical studies by Hern [11] based on Frittelli-Reula formulation [12], and by the authors [13] based on Ashtekar’s formulation [14, 15, 16][31]. Therefore we may say that the mathematical notion of “hyperbolicity” is not always applicable for predicting the stability of numerical integration of the Einstein equations. It will be useful if we have alternative procedure to predict the stability including the effect of the non-principal parts of the equation, which is neglected in the discussion of the hyperbolicity.

The third is to construct a robust system against the violation of the constraints, such as the constraint surface is the attractor. The idea was first proposed as “ $\lambda$ -system” by Brodbeck et al [19] in which they introduce artificial flow to the constraint surface using a new variable based on the symmetric hyperbolic system. This idea was tested and was confirmed to work as expected in some test simulations by the authors[20] (based on the formulation developed by [21]). Although there is a problem whether the recovered solution is the true evolution or not [22], we think that to enforce the decay of errors in its initial perturbative stage is the key to the next improvements. Actually, by

---

\*Electronic address: shinkai@atlas.riken.go.jp

†Electronic address: yoneda@mn.waseda.ac.jp

studying the evolution equations of the constraints (here after we call them constraint propagation) and by evaluating eigenvalues (amplification factors, AFs) of constraint propagation in its homogenized form, we found that the similar “asymptotically constrained system” can be obtained by simply adjusting constraints to the evolution equations, even for the ADM equations [23].

The purpose of this article is to extend our previous study [23] in more general expressions and also to apply the systems to a curved spacetime. Adjusting evolution equations is not the new idea. Actually the standard ADM system for numerical relativists [2] is adjusted from the original one [1] using the Hamiltonian constraint (See Frittelli’s analysis on constraint propagation between two [24]). Detweiler [25] proposed a system using adjustments so as that the L2 norm of constraints may not blow up (that we will study later in detail). Several numerical relativity groups recently report the advantages of the adjusting procedure with a successful example [8, 9]. We here try to understand the background mathematical features systematically by using AFs of constraint propagation.

We conjecture that we can construct an asymptotically constrained system by evaluating the AFs in advance. Especially, we propose that if the amplification factors are negative or pure-imaginary, then the system becomes stabler. This conjecture is already approved by numerical studies [20] in the Maxwell equations and in the Ashtekar version of the Einstein equations on the Minkowskii background. In this article, we show when and where such a feature is available using the ADM equations for Schwarzschild spacetime. We believe that this study clarifies the properties of adjustments and indicates further possibilities.

The section II is for describing our idea of “adjusted systems” generally, and the application to the ADM formulation. We then explain how we calculate the “amplification factors” in the spherically symmetric spacetime in §III, and show several examples in §IV. The concluding remark is in §V. Appendix A summarizes the constraint propagation equations of the ADM formulation generally, which may be useful for further studies. Appendix B briefly explains a way to obtain maximally sliced Schwarzschild spacetime that is used to obtain Fig.8.

## II. ADJUSTED SYSTEMS

### A. Procedure and background – general discussion –

We begin overviewing the adjusting procedure and the idea of the background structure, which were described in our previous works [20, 23].

Suppose we have a set of dynamical variables  $u^a(x^i, t)$ , and their evolution equations

$$\partial_t u^a = f(u^a, \partial_i u^a, \dots), \quad (2.1)$$

and the (first class) constraints

$$C^\alpha(u^a, \partial_i u^a, \dots) \approx 0. \quad (2.2)$$

For monitoring the violation of constraints, we propose to investigate the evolution equation of  $C^\alpha$  (constraint propagation),

$$\partial_t C^\alpha = g(C^\alpha, \partial_i C^\alpha, \dots). \quad (2.3)$$

(We do not mean to integrate (2.3) numerically, but to evaluate analytically in advance.) Then, there may be two major analysis on (2.3); (a) the hyperbolicity of (2.3) if (2.3) forms a first order form, and (b) the eigenvalue analysis of whole RHS terms in (2.3) after certain adequate homogenized procedure.

The hyperbolicity analysis is well-established, and necessary procedure if the evolution equations form a first-order system. The analysis mainly for identifying the level of hyperbolicity and the characteristic speed of the system, that are from eigenvalues of the principal matrix. We expect mathematically rigorous well-posed features for strongly or symmetric hyperbolic systems, and the characteristic speeds suggest us the satisfactory criteria for stable evolutions if they are real, under the propagation speed of the original variables,  $u^a$ , and/or within the causal region of a numerical integration scheme that is applied.

However, the hyperbolicity analysis can be applied only for the first-order system. For example, the evolution equations of the standard/original ADM formulation, (2.1), does not form a first-order, while their constraint propagation equations, (2.3), form the first-order by luck. If one adjust ADM equations with constraints, then this first-order characters will not be guaranteed. Another problem in the hyperbolic analysis is that it only discusses the principal part of the system, and ignore the rest. If there is a method to characterize the non-principal part, then that will help our understanding of the stability more clearly.

The second analysis, the eigenvalue analysis of whole RHS terms in (2.3), may compensate above problems. We propose to homogenize (2.3) by a Fourier transformation, e.g.

$$\begin{aligned}\partial_t \hat{C}^\alpha &= \hat{g}(\hat{C}^\alpha) = M^\alpha{}_\beta \hat{C}^\beta, \\ \text{where } C(x, t)^\rho &= \int \hat{C}(k, t)^\rho \exp(ik \cdot x) d^3k,\end{aligned}\tag{2.4}$$

then to analyze the set of eigenvalues, say  $\Lambda$ s, of the coefficient matrix,  $M^\alpha{}_\beta$ , in (2.4). We call  $\Lambda$ s the amplification factors (AFs) of (2.3). As we have proposed and confirmed in [20]:

**Conjecture:** *if the amplification factors*

(a) *have negative real-part (the constraints are forced to be diminished), or*

(b) *are non-zero (pure-imaginary) eigenvalues (the constraints are propagating away),*

*then we see more stable evolutions than the system which has positive or zero amplification factors.*

We found heuristically that the system become stabler when as much  $\Lambda$ s satisfies the above criteria and/or as large magnitude of  $\Lambda$ s away from zeros. We remark that this eigenvalue analysis requires to fix a particular background spacetime, since the AFs depends on the dynamical variables,  $u^a$ .

The above features of the constraint propagation, (2.3), will differ when we modify the original evolution equations. Suppose we add (adjust) the evolution equations using constraints

$$\partial_t u^a = f(u^a, \partial_i u^a, \dots) + F(C^\alpha, \partial_i C^\alpha, \dots),\tag{2.5}$$

then (2.3) will also be modified as

$$\partial_t C^\alpha = g(C^\alpha, \partial_i C^\alpha, \dots) + G(C^\alpha, \partial_i C^\alpha, \dots).\tag{2.6}$$

Therefore, the problem is how to adjust the evolution equations so as to their constraint propagations satisfy the above criteria as much as possible.

## B. Standard ADM system and its constraint propagation

We start by analyzing the standard ADM system. By “standard ADM” we mean here the most widely adopted system, due to York [2], with the evolution equations,

$$\partial_t \gamma_{ij} = -2\alpha K_{ij} + \nabla_i \beta_j + \nabla_j \beta_i,\tag{2.7}$$

$$\begin{aligned}\partial_t K_{ij} &= \alpha R_{ij}^{(3)} + \alpha K K_{ij} - 2\alpha K_{ik} K^k{}_j - \nabla_i \nabla_j \alpha \\ &\quad + (\nabla_i \beta^k) K_{kj} + (\nabla_j \beta^k) K_{ki} + \beta^k \nabla_k K_{ij},\end{aligned}\tag{2.8}$$

and the constraint equations,

$$\mathcal{H} := R^{(3)} + K^2 - K_{ij} K^{ij},\tag{2.9}$$

$$\mathcal{M}_i := \nabla_j K^j{}_i - \nabla_i K,\tag{2.10}$$

where  $(\gamma_{ij}, K_{ij})$  are the induced three-metric and the extrinsic curvature,  $(\alpha, \beta_i)$  are the lapse function and the shift covector,  $\nabla_i$  is the covariant derivative adapted to  $\gamma_{ij}$ , and  $R_{ij}^{(3)}$  is the three-Ricci tensor.

The constraint propagation equations, which are the time evolution equations of the Hamiltonian constraint (2.9) and the momentum constraints (2.10), can be written as

$$\begin{aligned}\partial_t \mathcal{H} &= \beta^j (\partial_j \mathcal{H}) + 2\alpha K \mathcal{H} - 2\alpha \gamma^{ij} (\partial_i \mathcal{M}_j) \\ &\quad + \alpha (\partial_l \gamma_{mk}) (2\gamma^{ml} \gamma^{kj} - \gamma^{mk} \gamma^{lj}) \mathcal{M}_j - 4\gamma^{ij} (\partial_j \alpha) \mathcal{M}_i,\end{aligned}\tag{2.11}$$

$$\begin{aligned}\partial_t \mathcal{M}_i &= -(1/2)\alpha (\partial_i \mathcal{H}) - (\partial_i \alpha) \mathcal{H} + \beta^j (\partial_j \mathcal{M}_i) \\ &\quad + \alpha K \mathcal{M}_i - \beta^k \gamma^{jl} (\partial_i \gamma_{lk}) \mathcal{M}_j + (\partial_i \beta_k) \gamma^{kj} \mathcal{M}_j.\end{aligned}\tag{2.12}$$

Another expressions of these constraint propagations are introduced in the Appendix A of this article.

### C. Adjustment to ADM dynamical equations and its effects to the constraint propagations

Generally, we can write the adjustment terms to (2.7) and (2.8) using (2.9) and (2.10) by the following combinations (using up to the first derivative of constraints for simplicity),

$$\text{adjustment term of } \partial_t \gamma_{ij} : \quad +P_{ij}\mathcal{H} + Q^k_{ij}\mathcal{M}_k + p^k_{ij}(\nabla_k \mathcal{H}) + q^{kl}_{ij}(\nabla_k \mathcal{M}_l), \quad (2.13)$$

$$\text{adjustment term of } \partial_t K_{ij} : \quad +R_{ij}\mathcal{H} + S^k_{ij}\mathcal{M}_k + r^k_{ij}(\nabla_k \mathcal{H}) + s^{kl}_{ij}(\nabla_k \mathcal{M}_l), \quad (2.14)$$

where  $P, Q, R, S$  and  $p, q, r, s$  are multipliers (please do not confuse  $R_{ij}$  with three Ricci curvature that we write as  $R^{(3)}_{ij}$ ).

According to this adjustment, the constraint propagation equations are also modified as

$$\partial_t \mathcal{H} = (2.11) + H_1^{mn}(2.13) + H_2^{imn}\partial_i(2.13) + H_3^{ijmn}\partial_i\partial_j(2.13) + H_4^{mn}(2.14), \quad (2.15)$$

$$\partial_t \mathcal{M}_i = (2.12) + M_{1i}^{mn}(2.13) + M_{2i}^{jmn}\partial_j(2.13) + M_{3i}^{mn}(2.14) + M_{4i}^{jmn}\partial_j(2.14). \quad (2.16)$$

with appropriate changes in indices. (See detail in the appendix A. The definitions of  $H_1, \dots, M_1, \dots$  are also there.)

### D. Examples of adjustments

We show several examples of adjustments here.

The first to test is to show the differences between the standard ADM [2] and the original ADM system [1]. In terms of (2.13) and (2.14), the adjustment,

$$R_{ij} = \kappa_F \alpha \gamma_{ij}, \quad (2.17)$$

will distinguish two, where  $\kappa_F$  is a constant and set other multiplier zero. Here  $\kappa_F = 0$  corresponds to the standard ADM (no adjustment), and  $\kappa_F = -1/4$  to the original ADM (without any adjustment to the canonical formulation by ADM). As one can check the adjusted constraint propagation equations in the appendix A, adding  $R_{ij}$  term keeps the constraint propagation in a first-order form. Frittelli [24] (see also [23]) pointed out that the hyperbolicity of constraint propagation equations is better in the standard ADM system.

The second example should be the one proposed by Detweiler [25]. He found that with a particular combination (see below), the evolution of the energy norm of the constraints,  $\mathcal{H}^2 + \mathcal{M}^2$ , can be negative definite when we apply the maximal slicing condition,  $K = 0$ . His adjustment can be written in our notation in (2.13) and (2.14), as

$$P_{ij} = -\kappa_L \alpha^3 \gamma_{ij}, \quad (2.18)$$

$$R_{ij} = \kappa_L \alpha^3 (K_{ij} - (1/3)K\gamma_{ij}), \quad (2.19)$$

$$S^k_{ij} = \kappa_L \alpha^2 [3(\partial_i \alpha) \delta^k_j - (\partial_l \alpha) \gamma_{ij} \gamma^{kl}], \quad (2.20)$$

$$s^{kl}_{ij} = \kappa_L \alpha^3 [\delta^k_i \delta^l_j - (1/3)\gamma_{ij} \gamma^{kl}], \quad (2.21)$$

everything else zero, where  $\kappa_L$  is a constant. Detweiler's adjustment, (2.18)-(2.21), does not put constraint propagation equation to a first order form, so we can not discuss hyperbolicity or the characteristic speed of the constraints. We confirmed numerically, using perturbation on Minkowski spacetime, that Detweiler's system presents better accuracy than the standard ADM, but only for small positive  $\kappa_L$ . See the Appendix of [23].

The ways of adjustments, actually, exist infinitely. Actually one of our criteria, the negative real AFs, requires to break the time-symmetric features of the standard ADM system (when we apply to the time-symmetric background metric). One observation by us [23] is that such AFs are available if we adjust the terms which break the time reversal symmetry of the evolution equations. That is, by reversing the time ( $\partial_t \rightarrow -\partial_t$ ), there are variables which change their signatures  $[K_{ij}, \partial_t \gamma_{ij}, \mathcal{M}_i, \dots]$ , while they are not  $[g_{ij}, \partial_t K_{ij}, \mathcal{H}, \dots]$ . (Here we are assuming the 3-metric  $\gamma_{ij}$  has the plus parity for the time reversal symmetry). So that the multiplier, for example,  $P_{ij}$  in (2.13) is desired to have plus parity in order to break the minus parity of  $\partial_t \gamma_{ij}$  equation.

We list up several combinations of adjustments in Table I and Table III. (Table I shows the ones we have plots, and the list of plots is in Table II). We defined the adjustments so as their positive multiplier parameter,  $\kappa > 0$ , makes the system *better* stability properties. (Here *better* means along to our conjecture in §II A). In this article, we do not discuss the ranges of the effective multiplier parameter,  $\kappa$ , since the range is depend on the characteristic speeds of the models and numerical integration schemes as we observed in [20].

We show how they affect in Schwarzschild spacetime in §IV.

### III. CONSTRAINT PROPAGATIONS IN SPHERICALLY SYMMETRIC SPACETIME

From here, we restrict our discussion to spherically symmetric spacetime. We introduce the violation of constraints as its perturbation around zero using harmonics. According to our motivation, the actual procedure to analyze the adjustments is to substitute the perturbed metric to the (adjusted) evolution equations first and to evaluate the according perturbative errors in the (adjusted) constraint propagation equations. However, for simplicity, we apply the perturbation to the pair of constraints directly and analyze the effects of adjustments in its propagation equations. The latter, we think, presents the feature of constraint propagation more clearly for our purposes.

#### A. The procedure

The discussion becomes clear if we expand the constraint  $C_\mu := (\mathcal{H}, \mathcal{M}_i)^T$  using vector harmonics,

$$C_\mu = \sum_{l,m} (A^{lm} a_{lm} + B^{lm} b_{lm} + C^{lm} c_{lm} + D^{lm} d_{lm}), \quad (3.1)$$

where we choose the basis as

$$a_{lm}(\theta, \varphi) = (Y_{lm}, 0, 0, 0)^T, \quad (3.2)$$

$$b_{lm}(\theta, \varphi) = (0, Y_{lm}, 0, 0)^T, \quad (3.3)$$

$$c_{lm}(\theta, \varphi) = \frac{r}{\sqrt{l(l+1)}} (0, 0, \partial_\theta Y_{lm}, \partial_\varphi Y_{lm})^T, \quad (3.4)$$

$$d_{lm}(\theta, \varphi) = \frac{r}{\sqrt{l(l+1)}} (0, 0, -\frac{1}{\sin \theta} \partial_\varphi Y_{lm}, \sin \theta \partial_\theta Y_{lm})^T, \quad (3.5)$$

and the coefficients  $A^{lm}, \dots, D^{lm}$  are functions of  $(t, r)$ . Here  $Y_{lm}$  is the spherical harmonic function,

$$Y_{lm}(\theta, \varphi) = (-1)^{(m+|m|)/2} \sqrt{\frac{(2l+1)}{4\pi} \frac{(l-|m|)!}{(l+|m|)!}} P_l^m(\cos \theta) e^{im\varphi}. \quad (3.6)$$

The basis (3.2)-(3.5) are normalized so that they satisfy

$$\langle C_\mu, C_\nu \rangle = \int_0^{2\pi} d\varphi \int_0^\pi C_\mu^* C_\nu \eta^{\mu\rho} \sin \theta d\theta, \quad (3.7)$$

where  $\eta^{\mu\rho}$  is Minkowskii metric and the asterisk denotes the complex conjugate. Therefore

$$A^{lm} = \langle a_{lm}, C_\nu \rangle, \quad \partial_t A^{lm} = \langle a_{lm}, \partial_t C_\nu \rangle, \quad \text{etc.} \quad (3.8)$$

In order to analyze the radial dependences, we also express these evolution equations using the Fourier expansion on the radial coordinate,

$$A^{lm} = \sum_k \hat{A}_{(k)}^{lm}(t) e^{ikr} \quad \text{etc.} \quad (3.9)$$

So that we will be able to obtain the RHS of the evolution equations for  $(\hat{A}_{(k)}^{lm}(t), \dots, \hat{D}_{(k)}^{lm}(t))^T$  in a homogeneous form.

#### B. Expression for the standard ADM formulation

We write the spherically symmetric spacetime using a metric,

$$ds^2 = -(\alpha(t, r)^2 - \beta_r(t, r)^2 / \gamma_{rr}) dt^2 + 2\beta_r(t, r) dt dr + \gamma_{rr}(t, r) dr^2 + \gamma_{\theta\theta}(t, r) (d\theta^2 + \sin^2 \theta d\varphi^2), \quad (3.10)$$

where  $\alpha$  and  $\beta_r$  are the lapse function and the shift vector.  $\gamma_{rr}$  and  $\gamma_{\theta\theta}$  are also interpreted as 3-metric in 3+1 decomposition, so that the relevant extrinsic curvature,  $K_{ij}$ , become  $K_{ij} = \text{diag}(K_{rr}, K_{\theta\theta}, K_{\theta\theta} \sin^2 \theta)$  and its trace becomes  $K = K_{rr}/\gamma_{rr} + 2K_{\theta\theta}/\gamma_{\theta\theta}$ .

According to the procedure in the previous section, we obtain the constraint propagation equations for the standard ADM formulation, (2.11) and (2.12), in the following form:

$$\begin{aligned} \partial_t A^{lm}(t, r) = & 2\alpha K A^{lm} + \beta^r (\partial_r A^{lm}) \\ & - 2\alpha \gamma^{rr} (\partial_r B^{lm}) + (\alpha (\partial_r \gamma_{rr}) \gamma^{rr} \gamma^{rr} - 2\alpha (\partial_r \gamma_{\theta\theta}) \gamma^{\theta\theta} \gamma^{rr} - 4\gamma^{rr} (\partial_r \alpha)) B^{lm} \\ & - 2\alpha \gamma^{\theta\theta} r \sqrt{l(l+1)} C^{lm}, \end{aligned} \quad (3.11)$$

$$\begin{aligned} \partial_t B^{lm}(t, r) = & -(1/2)\alpha \partial_r A^{lm} - (\partial_r \alpha) A^{lm} \\ & + (\alpha K - \beta^r \gamma^{rr} (\partial_r \gamma_{rr}) + (\partial_r \beta_r) \gamma^{rr}) B^{lm} + \beta^r \partial_r B^{lm}, \end{aligned} \quad (3.12)$$

$$\partial_t C^{lm}(t, r) = -\frac{\alpha \sqrt{l(l+1)}}{2r} A^{lm} + \alpha K C^{lm} + \beta^r \left( \frac{1}{r} C^{lm} + \partial_r C^{lm} \right), \quad (3.13)$$

$$\partial_t D^{lm}(t, r) = \alpha K D^{lm} + \beta^r \left( \frac{1}{r} D^{lm} + \partial_r D^{lm} \right), \quad (3.14)$$

and then

$$\begin{aligned} \frac{d}{dt} \hat{A}_{(k)}^{lm}(t) = & (2\alpha K + ik\beta^r) \hat{A}_{(k)}^{lm} \\ & + (-2ik\alpha \gamma^{rr} + \alpha (\partial_r \gamma_{rr}) \gamma^{rr} \gamma^{rr} - 2\alpha (\partial_r \gamma_{\theta\theta}) \gamma^{\theta\theta} \gamma^{rr} - 4\gamma^{rr} (\partial_r \alpha)) \hat{B}_{(k)}^{lm} \\ & - 2\alpha \gamma^{\theta\theta} r \sqrt{l(l+1)} \hat{C}_{(k)}^{lm}, \end{aligned} \quad (3.15)$$

$$\frac{d}{dt} \hat{B}_{(k)}^{lm}(t) = (-ik/2)\alpha - (\partial_r \alpha) \hat{A}_{(k)}^{lm} + (\alpha K - \beta^r \gamma^{rr} (\partial_r \gamma_{rr}) + (\partial_r \beta_r) \gamma^{rr} + ik\beta^r) \hat{B}_{(k)}^{lm}, \quad (3.16)$$

$$\frac{d}{dt} \hat{C}_{(k)}^{lm}(t) = -\frac{\alpha \sqrt{l(l+1)}}{2r} \hat{A}_{(k)}^{lm} + (\alpha K + \frac{\beta^r}{r} + ik\beta^r) \hat{C}_{(k)}^{lm}, \quad (3.17)$$

$$\frac{d}{dt} \hat{D}_{(k)}^{lm}(t) = (\alpha K + \frac{\beta^r}{r} + ik\beta^r) \hat{D}_{(k)}^{lm}. \quad (3.18)$$

There is no dependence on  $m$ . We see the expressions are equivalent with the case of the flat background spacetime [23] when we take  $l = 0$  and  $r \rightarrow \infty$ . Therefore our results also show the behaviour of the flat background limit in its large  $r$  limit.

### C. Example: original ADM formulation

We only present here one example, the comparison between the standard and original ADM systems. By substituting (2.17) into (2.15) and (2.16), we obtain

$$\partial_t \mathcal{H} = (2.11) + 4\kappa_1 \alpha K \mathcal{H}, \quad (3.19)$$

$$\partial_t \mathcal{M}_i = (2.12) - 2\kappa_1 \alpha (\partial_i \mathcal{H}) - 2\kappa_1 (\partial_i \alpha) \mathcal{H}. \quad (3.20)$$

In the spherically symmetric spacetime, this adjustment affects to (3.11)-(3.14) as follows:

$$\partial_t A^{lm}(t, r) = (3.11) + 4\kappa_1 \alpha K A^{lm}, \quad (3.21)$$

$$\partial_t B^{lm}(t, r) = (3.12) - 2\kappa_1 \alpha \partial_r A^{lm} - 2\kappa_1 (\partial_r \alpha) A^{lm}, \quad (3.22)$$

$$\partial_t C^{lm}(t, r) = (3.13) - \frac{2\kappa_1 \alpha \sqrt{l(l+1)}}{r} A^{lm}, \quad (3.23)$$

$$\partial_t D^{lm}(t, r) = (3.14). \quad (3.24)$$

After the homogenization, (3.15)-(3.18) become

$$\frac{d}{dt} \begin{pmatrix} \hat{A}_{(k)}^{lm} \\ \hat{B}_{(k)}^{lm} \\ \hat{C}_{(k)}^{lm} \\ \hat{D}_{(k)}^{lm} \end{pmatrix} = \begin{pmatrix} (3.15) \\ (3.16) \\ (3.17) \\ (3.18) \end{pmatrix} + \begin{pmatrix} 4\kappa_1 \alpha K & 0 & 0 & 0 \\ -2\kappa_1 \alpha ik & -2\kappa_1 (\partial_r \alpha) & 0 & 0 & 0 \\ -2\kappa_1 \alpha \sqrt{l(l+1)}/r & 0 & 0 & 0 & 0 \\ 0 & 0 & 0 & 0 & 0 \end{pmatrix} \begin{pmatrix} \hat{A}_{(k)}^{lm} \\ \hat{B}_{(k)}^{lm} \\ \hat{C}_{(k)}^{lm} \\ \hat{D}_{(k)}^{lm} \end{pmatrix}. \quad (3.25)$$

The eigenvalues (AFs)  $\Lambda^i$  of the RHS matrix of (3.25) can be calculated by fixing the metric components including the gauge. For example, on the standard Schwarzschild metric (4.1), they are

$$\begin{aligned}\Lambda^i &= (0, 0, \sqrt{a}, -\sqrt{a}) \\ a &= -k^2 + \frac{4Mk^2r^2(r-M) + 2M(2r-M) + l(l+1)r(r-2M) + ikr(2r^2-3Mr-2M^2)}{r^4}\end{aligned}\quad (3.26)$$

for the choice of  $\kappa_1 = 0$  (the standard ADM), while they are

$$\Lambda^i = (0, 0, \sqrt{b}, -\sqrt{b}), \quad b = \frac{M(2r-M) + irkM(2M-r)}{r^4}\quad (3.27)$$

for the choice of  $\kappa_1 = -1/4$  (the original ADM).

#### D. Our analytic approach

The above example is the simplest one. In the next section, we will show the AFs of the adjusted systems shown in the Table I, there analytical expressions are mostly too long to write down. We therefore will plot AFs to see if the real parts go negative, or if the imaginary parts go non-zero or not.

We used the symbolic calculation softwares both *Mathematica* and *Maple*, and made plots by checking two independent outputs. These scripts are available upon requests.

### IV. CONSTRAINT PROPAGATIONS IN SCHWARZSCHILD SPACETIME

#### A. Coordinates

We present our analysis of the constraint propagation equations in the Schwarzschild black hole spacetime,

$$ds^2 = -(1 - \frac{2M}{r})dt^2 + \frac{dr^2}{1 - 2M/r} + r^2d\Omega^2, \quad (\text{the standard expression}) \quad (4.1)$$

where  $M$  is the mass of a black hole. For numerical relativists, evolving a single black hole is the necessary test problem, though it is a trivial at first sight. The standard expression, (4.1), has a coordinate singularity at  $r = 2M$ , so that we need to move another coordinate for an actual numerical time integrations.

One alternative is the isotropic coordinate,

$$ds^2 = -(\frac{1 - M/2r_{iso}}{1 + M/2r_{iso}})^2 dt^2 + (1 + \frac{M}{2r_{iso}})^4 [dr_{iso}^2 + r_{iso}^2 d\Omega^2], \quad (\text{the isotropic expression}) \quad (4.2)$$

which is given by the coordinate transformation,  $r = (1 + M/2r_{iso})^2 r_{iso}$ . Here  $r_{iso} = M/2$  indicates the minimum throat radius of the Einstein-Rosen bridge. Bernstein, Hobill and Smarr [26] showed a systematic comparisons for numerical integration schemes applying the coordinate transformation,  $r_{iso} = Me^{r_{new}}/2$ , further to (4.2).

The expression of the ingoing Eddington-Finkelstein (iEF) coordinate become somewhat popular in numerical relativity for treating black hole boundaries as an excision, since iEF penetrates the horizon without a coordinate singularity. The expression is,

$$ds^2 = -(1 - \frac{2M}{r})dt_{iEF}^2 + \frac{4M}{r}dt_{iEF}dr + (1 + \frac{2M}{r})dr^2 + r^2d\Omega^2 \quad (\text{the iEF expression}) \quad (4.3)$$

which is given by  $t_{iEF} = t + 2M \log(r - 2M)$  and the radial coordinate is common to (4.1). The geometrical interpretation of the iEF coordinate system is that in addition to having a timelike killing vector, the combination of timelike and radial tangent vectors  $\vec{\partial}_t - \vec{\partial}_r$  remains null.

Another expression we test is the Painlevé-Gullstrand (PG) coordinates,

$$ds^2 = -\left(1 - \frac{2M}{r}\right)dt_{PG}^2 + 2\sqrt{\frac{2M}{r}}dt_{PG}dr + dr^2 + r^2d\Omega^2, \quad (\text{the PG expression}) \quad (4.4)$$

which is given by  $t_{PG} = t + \sqrt{8Mr} - 2M \log\{(\sqrt{r/2M} + 1)/(\sqrt{r/2M} - 1)\}$  and the radial coordinate is common to (4.1). The PG coordinate system can be viewed as that anchored to a family of freely moving observers (time-like) starting at infinity with vanishing velocity [27].

The latter two (iEF/PG) are also different from the former (standard/isotropic) two in the point that their extrinsic curvature on the initial slice ( $t_{iEF} = t_{PG} = 0$ ) is not zero. To conclude first, the effects of adjustments are similar between the formers and between the latters.

In Table. II, we list up the combinations (adjustments and coordinates) we plotted.

### B. in the standard Schwarzschild coordinate

We first show the case of the standard Schwarzschild coordinate, (4.1), since this example gives us the basic overview of our analysis. The cases of the isotropic coordinate, (4.2), will be shown quite similar.

In Fig.1(a), the amplification factors (AFs, the eigenvalues of homogenized constraint propagation equations) of the standard ADM formulation are plotted. The solid lines and dotted lines with circles are real parts and imaginary parts of AFs, respectively. (The figure style is common through out the article.) They are four lines each, but as we showed in (3.26), two of them are zero. The plotting range is  $2 < r \leq 20$  in Schwarzschild radial coordinate. The AFs at  $r = 2$  are  $\pm\sqrt{3/8}$  and 0. The existence of this positive real AF near the horizon is new result which was not seen in the flat background [23]. We show only the cases with  $l = 2$  and  $k = 1$ , because we judged the plots of  $l = 0$  and other  $k$ s are qualitatively the same.

The adjustment (2.17) with  $\kappa_F = -1/4$  makes the system back to the original ADM. AFs are (3.27) and we plot them in Fig.1(b). We see the imaginary parts are apparently different from those of the standard ADM [Fig.1(a)]. This is the same feature with the case of flat background [23]. According to our conjecture, the non-zero imaginary values is better than zeros, so that we expect the standard ADM has better stability feature than the original ADM system. Negative  $\kappa_F$  makes the asymptotical real values finite. If we change the signature of  $\kappa_F$ , then AFs are as in Fig.1(c). The imaginary parts become larger than  $\kappa_F = 0$ , that indicates the constraint propagation involves higher frequency modes.

The adjustment proposed by Detweiler, (2.18)-(2.21), makes the feature completely different. Fig.2(a) and (b) are the case of  $\kappa_L = 1/4$  and  $1/2$  and (c) is of the different signature of  $\kappa_L$ . The great improvement can be seen in both positive  $\kappa_L$  cases that *all* real parts are become negative in large  $r$ . Moreover all imaginary parts are apart from zero. These are the desired features according to our conjecture. Therefore we expect the Detweiler adjustment has good stability properties *except* the near black hole region. The AF near the horizon *has* positive real component, which is not a good news. Detweiler's original idea came from suppressing the *total* L2 norm of constraints on the spatial slice. Our plot indicates that the existence of the *local* violation mode. The change of signature of  $\kappa_L$  can be understood just the change of signature of AFs, and this fact can be seen also to the other examples.

We next show that the partial adjustments of Detweiler's are also not-so-bad. Fig.3 (a), (b) and (c) are the cases of adjustment that are of only (2.18), (2.20) and (2.21), respectively. [The contribution of (2.19) is none since  $K_{ij} = 0$  in the Schwarzschild coordinate.] By comparing them with Fig.1(a) and Fig.2(b), we see the negative real parts in large  $r$  are originated by (2.18) and (2.21), while the former keeps two real parts remain zero. Fig.3(d) used only  $P_{ij} = -\kappa_L \alpha \gamma_{ij}$  and else zero, which is a minor modification from (2.18). The contribution is similar, and can be said *effective*.

### C. in isotropic/iEF/PG coordinates

We next compare AFs between different coordinate expressions. The first test is for the standard ADM formulation. Fig.4 shows AFs for (a) the isotropic coordinate (4.2), (b) the iEF coordinate (4.3), and (c) the PG coordinate (4.4). All plots are on the time slice of  $t = 0$  in each coordinate expression. [See Fig.1(a) for the standard Schwarzschild coordinate.] We see that Fig.1(a) and Fig.4(a) are quite similar, while Fig.4(b) and (c) are qualitatively different from the formers. This is because the latter expressions (iEF/PG) are asymmetric according to time, i.e. they have non-zero extrinsic curvature.

We note that the constraint propagation equations are invariant for spatial coordinate transformation, but AFs are invariant only for their linear transformation. This explains why there is differences between Fig.1(a) and Fig.4(a), though not significant.

We notice that some AFs in iEF/PG are remain positive [Fig.4(b) and (c)] in large  $r$  region, that nature however will change due to the adjustments. Fig.5 is for the Detweiler-type adjustment, (2.18)-(2.21), for the isotropic/iEF/PG coordinate cases. [See Fig.2(b) for the standard Schwarzschild coordinate.] Interestingly, all plots indicates that all real parts of AFs are negative, and imaginary parts are non-zero (again except the near black hole region). By



arranging the multiplier parameter, for the iEF/PG coordinates, there is a chance to get all negative real AFs outside of the black hole horizon.

Fig.6 is for the simplified adjustment of Detweiler's (see No.3 in Table.I). As we saw in Fig.3(d) for the standard Schwarzschild coordinate case, this version also works as desired. The two real parts for the isotropic coordinate case remain zero which is the same as before, and they are asymptotically zero for iEF/PG, but other characters are similar to the original ones.

Fig.7 is for the adjustment No.4 in Table. I, which was used in the test of PennState group [9]. The main difference from above is that the adjustment here is only for the radial component of the extrinsic curvature,  $K_{rr}$ . The numerical experiments in [9] show better stability for positive  $\kappa_\mu$ , that fact can be seen also from Fig.7: positive  $\kappa_\mu$  produces negative real AFs. [See Fig.4(b)(c) for the standard ADM case.]

Such kinds of test can be done with other combinations. In Table.III, we listed our results for more examples. The table includes the above results and is intended to extract the contributions of the each term in (2.13) and (2.14). The effects of adjustments (of each  $\kappa > 0$  case) to AFs are commented for each coordinate system and for real/imaginary parts of AFs, respectively. These judgements are made at the  $r \sim O(10M)$  region on their  $t = 0$  slice. We hope this table will help further numerical improvements for the community.

#### D. in maximally-sliced evolving Schwarzschild spacetime

So far, our discussion is limited to on one 3-hypersurface. Generally speaking, such an initial-value like analysis may not be enough to determine what combination of adjustments, coordinate system, and gauge conditions are good or not for numerical evolution problem. Here as the first further step, we show our analysis on several snapshots of maximally sliced Schwarzschild spacetime.

The so-called maximal slicing condition,  $K = 0$ , is one of the most widely used gauge condition to fix the lapse function,  $\alpha$ , during numerical evolution, since it has a feature of singularity avoidance. The condition will turn to an elliptic equation for  $\alpha$ . However, for the case of Schwarzschild spacetime, we can express a maximally-sliced hypersurface at an arbitrary time without full numerical time integration. The recipe is given by Estabrook et al [28], and we introduce the procedure briefly in the Appendix B.

By specifying a particular time  $\bar{t}$ , where  $\bar{t}$  is supposed to express the time coordinate on a maximally sliced hypersurface (see detail in Appendix B), we get metric components ( $\alpha, \beta$  and  $\gamma_{ij}$ ). The procedure requires us to solve ODE, but it is not a result of time integration. We then calculate AFs common to the previous ones.

We show several snapshots in Fig.8. We picked up the slices of  $\bar{t} = 0, 1, 2, \dots, 5$  for (a) the standard ADM, (b) the original ADM, and (c) Detweiler-type adjustment for the Schwarzschild coordinate. These initial data ( $\bar{t} = 0$ ) is the same with Fig.1(a), (b) and Fig.2(b), respectively. It is well known that the maximally-sliced hypersurfaces approach (or stop approaching to the singularity)  $r_{min} \rightarrow (3/2)M$  as  $\bar{t} \rightarrow \infty$ . The snapshots here corresponds to  $r_{min} = 2.00, 1.90, 1.76, 1.66, 1.60$  and  $1.56$  in unit of  $M$ .

The figures show that AFs are changing along the evolution though not drastically, and their evolution behavior is depend also on the choice of adjustments. The evolution makes the AFs' configuration converge, which is expected from the nature of the maximal slicing.

#### V. CONCLUDING REMARKS

In order to construct an asymptotically constrained evolution system, we proposed to adjust evolution equations by adding constraint terms by analyzing the constraint propagation equations in advance. This idea works even for the ADM formulation (which is not a hyperbolic system) against the flat background spacetime [23], and here we applied the similar studies to a curved spacetime, a spherically symmetric black hole spacetime.

Recently, several numerical relativity groups report the effects of adjustments and mostly they are searching a suitable combination of multipliers with trial and error. We hope our discussion here helps to understand the background mathematics systematically, though it may not be the perfect explanation. The most different point between our analysis and actual numerical studies is that this is the local analysis only on the evolution equations. The actual numerical results come together with the boundary conditions, the choice of numerical integration schemes, the grid structures, the accuracy of the initial data and so on. We think, however, that our proposal is an alternative to the hyperbolicity classification in the point that it includes the non-principal part of the evolution equations, and we expect that the discussion here provides the fundamental information of the stable formulation of the Einstein equations to the community.

We presented a useful expression for analyzing ADM constraint propagation in general in the Appendix A, and several analytic predictions of the adjustments for the Schwarzschild spacetime in Table. III. We searched when and

where the negative real or non-zero imaginary eigenvalues of the constraint propagation matrix appear, and how they depend on the choice of coordinate system and adjustments. Our analysis includes the proposal of Detweiler (1987), which is still the best one though it has a growing mode of constraint violation near the horizon.

We observed that the effects of adjustments depend on the choice of the coordinate, gauge conditions, and also on its time evolution. Therefore our basic assumption of the constancy of the multipliers may be better to be replaced with more general procedure in our future treatment. We already begin studying this direction by applying the recent development of the computational techniques in classical multibody dynamical systems [30], and hope that we can present some results soon in elsewhere.

### Acknowledgments

We thank Y. Erigushi, T. Harada, M. Shibata, M. Tiglio for helpful comments. HS is supported by the special postdoctoral researchers program at RIKEN.

## APPENDIX A: GENERAL EXPRESSIONS OF ADM CONSTRAINT PROPAGATION EQUATIONS

For the reader's convenience, we here express the constraint propagation equations generally, considering the adjustments to the dynamical equations. We repeat the necessary equations again in order to take this appendix independently.

### 1. The standard ADM equations and the constraint propagations

We start by analyzing the standard ADM system that is with evolution equations

$$\partial_t \gamma_{ij} = -2\alpha K_{ij} + \nabla_i \beta_j + \nabla_j \beta_i, \quad (\text{A1})$$

$$\begin{aligned} \partial_t K_{ij} = & \alpha R_{ij}^{(3)} + \alpha K K_{ij} - 2\alpha K_{ik} K^k_j - \nabla_i \nabla_j \alpha \\ & + (\nabla_i \beta^k) K_{kj} + (\nabla_j \beta^k) K_{ki} + \beta^k \nabla_k K_{ij}, \end{aligned} \quad (\text{A2})$$

and constraint equations

$$\mathcal{H} := R^{(3)} + K^2 - K_{ij} K^{ij}, \quad (\text{A3})$$

$$\mathcal{M}_i := \nabla_j K^j_i - \nabla_i K, \quad (\text{A4})$$

where  $(\gamma_{ij}, K_{ij})$  are the induced three-metric and the extrinsic curvature,  $(\alpha, \beta_i)$  are the lapse function and the shift covector,  $\nabla_i$  is the covariant derivative adapted to  $\gamma_{ij}$ , and  $R_{ij}^{(3)}$  is the three-Ricci tensor.

The constraint propagation equations, which are the time evolution equations of the Hamiltonian constraint (A3) and the momentum constraints (A4).

*a. Expression using  $\mathcal{H}$  and  $\mathcal{M}_i$*  The constraint propagation equations can be written as

$$\begin{aligned} \partial_t \mathcal{H} = & \beta^j (\partial_j \mathcal{H}) + 2\alpha K \mathcal{H} - 2\alpha \gamma^{ij} (\partial_i \mathcal{M}_j) \\ & + \alpha (\partial_l \gamma_{mk}) (2\gamma^{ml} \gamma^{kj} - \gamma^{mk} \gamma^{lj}) \mathcal{M}_j - 4\gamma^{ij} (\partial_j \alpha) \mathcal{M}_i, \end{aligned} \quad (\text{A5})$$

$$\begin{aligned} \partial_t \mathcal{M}_i = & -(1/2)\alpha (\partial_i \mathcal{H}) - (\partial_i \alpha) \mathcal{H} + \beta^j (\partial_j \mathcal{M}_i) \\ & + \alpha K \mathcal{M}_i - \beta^k \gamma^{jl} (\partial_i \gamma_{lk}) \mathcal{M}_j + (\partial_i \beta_k) \gamma^{kj} \mathcal{M}_j. \end{aligned} \quad (\text{A6})$$

This is a suitable form to discuss hyperbolicity of the system. The simplest derivation of (2.11) and (2.12) is by using the Bianchi identity, which can be seen in Frittelli [24].

A shorter expression is available, e.g.

$$\begin{aligned} \partial_t \mathcal{H} = & \beta^l \partial_l \mathcal{H} + 2\alpha K \mathcal{H} - 2\alpha \gamma^{-1/2} \partial_l (\sqrt{\gamma} \mathcal{M}^l) - 4(\partial_l \alpha) \mathcal{M}^l \\ = & \beta^l \nabla_l \mathcal{H} + 2\alpha K \mathcal{H} - 2\alpha (\nabla_l \mathcal{M}^l) - 4(\nabla_l \alpha) \mathcal{M}^l, \end{aligned} \quad (\text{A7})$$

$$\begin{aligned} \partial_t \mathcal{M}_i = & -(1/2)\alpha (\partial_i \mathcal{H}) - (\partial_i \alpha) \mathcal{H} + \beta^l \nabla_l \mathcal{M}_i + \alpha K \mathcal{M}_i + (\nabla_i \beta_l) \mathcal{M}^l \\ = & -(1/2)\alpha (\nabla_i \mathcal{H}) - (\nabla_i \alpha) \mathcal{H} + \beta^l \nabla_l \mathcal{M}_i + \alpha K \mathcal{M}_i + (\nabla_i \beta_l) \mathcal{M}^l, \end{aligned} \quad (\text{A8})$$

or by using Lie derivatives along  $\alpha n^\mu$ ,

$$\mathcal{L}_{\alpha n^\mu} \mathcal{H} = 2\alpha K \mathcal{H} - 2\alpha \gamma^{-1/2} \partial_t (\sqrt{\gamma} \mathcal{M}^l) - 4(\partial_t \alpha) \mathcal{M}^l, \quad (\text{A9})$$

$$\mathcal{L}_{\alpha n^\mu} \mathcal{M}_i = -(1/2)\alpha(\partial_t \mathcal{H}) - (\partial_i \alpha) \mathcal{H} + \alpha K \mathcal{M}_i. \quad (\text{A10})$$

*b. Expression using  $\gamma_{ij}$  and  $K_{ij}$*  In order to check the effects of the adjustments in (A1) and (A2) to the constraint propagation, it is useful to re-express (A5) and (A6) using  $\gamma_{ij}$  and  $K_{ij}$ . By a straightforward calculation, we obtain an expression as

$$\partial_t \mathcal{H} = H_1^{mn} (\partial_t \gamma_{mn}) + H_2^{imn} \partial_i (\partial_t \gamma_{mn}) + H_3^{ijmn} \partial_i \partial_j (\partial_t \gamma_{mn}) + H_4^{mn} (\partial_t K_{mn}), \quad (\text{A11})$$

$$\partial_t \mathcal{M}_i = M_{1i}^{mn} (\partial_t \gamma_{mn}) + M_{2i}^{jmn} \partial_j (\partial_t \gamma_{mn}) + M_{3i}^{mn} (\partial_t K_{mn}) + M_{4i}^{jmn} \partial_j (\partial_t K_{mn}), \quad (\text{A12})$$

where

$$H_1^{mn} := -2R^{(3)mn} - \Gamma_{kj}^p \Gamma_{pi}^k \gamma^{mi} \gamma^{nj} + \Gamma^m \Gamma^n \\ + \gamma^{ij} \gamma^{np} (\partial_i \gamma^{mk}) (\partial_j \gamma_{kp}) - \gamma^{mp} \gamma^{ni} (\partial_i \gamma^{kj}) (\partial_j \gamma_{kp}) - 2K K^{mn} + 2K^n_j K^{mj}, \quad (\text{A13})$$

$$H_2^{imn} := -2\gamma^{mi} \Gamma^n - (3/2) \gamma^{ij} (\partial_j \gamma^{mn}) + \gamma^{mj} (\partial_j \gamma^{in}) + \gamma^{mn} \Gamma^i, \quad (\text{A14})$$

$$H_3^{ijmn} := -\gamma^{ij} \gamma^{mn} + \gamma^{in} \gamma^{mj}, \quad (\text{A15})$$

$$H_4^{mn} := 2(K \gamma^{mn} - K^{mn}), \quad (\text{A16})$$

$$M_{1i}^{mn} := \gamma^{nj} (\partial_i K^m_j) - \gamma^{mj} (\partial_j K^n_i) + (1/2) (\partial_j \gamma^{mn}) K^j_i + \Gamma^n K^m_i, \quad (\text{A17})$$

$$M_{2i}^{jmn} := -\gamma^{mj} K^n_i + (1/2) \gamma^{mn} K^j_i + (1/2) K^{mn} \delta_i^j, \quad (\text{A18})$$

$$M_{3i}^{mn} := -\delta_i^n \Gamma^m - (1/2) (\partial_i \gamma^{mn}), \quad (\text{A19})$$

$$M_{4i}^{jmn} := \gamma^{mj} \delta_i^n - \gamma^{mn} \delta_i^j, \quad (\text{A20})$$

where we expressed  $\Gamma^m = \Gamma_{ij}^m \gamma^{ij}$ .

## 2. Adjustments

Generally, we here write the adjustment terms to (A1) and (A2) using (A3) and (A4) by the following combinations,

$$\text{adjustment term of } \partial_t \gamma_{ij} : \quad +P_{ij} \mathcal{H} + Q_{ij}^k \mathcal{M}_k + p_{ij}^k (\nabla_k \mathcal{H}) + q_{ij}^{kl} (\nabla_k \mathcal{M}_l), \quad (\text{A21})$$

$$\text{adjustment term of } \partial_t K_{ij} : \quad +R_{ij} \mathcal{H} + S_{ij}^k \mathcal{M}_k + r_{ij}^k (\nabla_k \mathcal{H}) + s_{ij}^{kl} (\nabla_k \mathcal{M}_l), \quad (\text{A22})$$

where  $P, Q, R, S$  and  $p, q, r, s$  are multipliers (please do not confuse  $R_{ij}$  with three Ricci curvature that we write as  $R_{ij}^{(3)}$ ).

By substituting above adjustments into (A11) and (A12), we can write the adjusted constraint propagation equations as

$$\begin{aligned} \partial_t \mathcal{H} = & \text{(original terms)} \\ & + H_1^{mn} [P_{mn} \mathcal{H} + Q_{mn}^k \mathcal{M}_k + p_{mn}^k (\nabla_k \mathcal{H}) + q_{mn}^{kl} (\nabla_k \mathcal{M}_l)] \\ & + H_2^{imn} \partial_i [P_{mn} \mathcal{H} + Q_{mn}^k \mathcal{M}_k + p_{mn}^k (\nabla_k \mathcal{H}) + q_{mn}^{kl} (\nabla_k \mathcal{M}_l)] \\ & + H_3^{ijmn} \partial_i \partial_j [P_{mn} \mathcal{H} + Q_{mn}^k \mathcal{M}_k + p_{mn}^k (\nabla_k \mathcal{H}) + q_{mn}^{kl} (\nabla_k \mathcal{M}_l)] \\ & + H_4^{mn} [R_{mn} \mathcal{H} + S_{mn}^k \mathcal{M}_k + r_{mn}^k (\nabla_k \mathcal{H}) + s_{mn}^{kl} (\nabla_k \mathcal{M}_l)], \end{aligned} \quad (\text{A23})$$

$$\begin{aligned} \partial_t \mathcal{M}_i = & \text{(original terms)} \\ & + M_{1i}^{mn} [P_{mn} \mathcal{H} + Q_{mn}^k \mathcal{M}_k + p_{mn}^k (\nabla_k \mathcal{H}) + q_{mn}^{kl} (\nabla_k \mathcal{M}_l)] \\ & + M_{2i}^{jmn} \partial_j [P_{mn} \mathcal{H} + Q_{mn}^k \mathcal{M}_k + p_{mn}^k (\nabla_k \mathcal{H}) + q_{mn}^{kl} (\nabla_k \mathcal{M}_l)] \\ & + M_{3i}^{mn} [R_{mn} \mathcal{H} + S_{mn}^k \mathcal{M}_k + r_{mn}^k (\nabla_k \mathcal{H}) + s_{mn}^{kl} (\nabla_k \mathcal{M}_l)] \\ & + M_{4i}^{jmn} \partial_j [R_{mn} \mathcal{H} + S_{mn}^k \mathcal{M}_k + r_{mn}^k (\nabla_k \mathcal{H}) + s_{mn}^{kl} (\nabla_k \mathcal{M}_l)]. \end{aligned} \quad (\text{A24})$$

Here the ‘‘original terms’’ can be understood either as (A5) and (A6), or as (A11) and (A12). Therefore, for example, we can see that the adjustments to  $\partial_t \gamma_{ij}$  does not always keep the constraint propagation equations in the first order form, due to their contribution in the third adjusted term in (A23).

We note that these expressions of constraint propagation equations are equivalent when we include the cosmological constant and/or matter terms.

## APPENDIX B: MAXIMALLY SLICING A SCHWARZSCHILD BLACK HOLE

The maximal slicing condition,  $K = 0$ , is one of the most widely used gauge condition to fix the lapse function,  $\alpha$ , during numerical evolution, since it has a feature of singularity avoidance. The condition will turn to an elliptic equation for  $\alpha$ , such as

$$\nabla^i \nabla_i \alpha = ({}^{(3)}R + K^2) \alpha = K_{ij} K^{ij} \alpha, \quad (\text{B1})$$

where we used the Hamiltonian constraint in the second equality. However, for the case of Schwarzschild spacetime, we can express a maximally-sliced hypersurface at an arbitrary time without full numerical integration. The recipe is given by Estabrook et al [28], and we introduce the procedure here briefly.

The goal is to express Schwarzschild geometry with a metric

$$ds^2 = (-\alpha^2 + A^{-1}\beta^2)d\bar{t}^2 + 2\beta d\bar{t}dr + A dr^2 + r^2(d\theta^2 + \sin^2\theta d\varphi^2), \quad (\text{B2})$$

where  $\alpha(\bar{t}, r)$ ,  $\beta(\bar{t}, r)$  and  $A(\bar{t}, r)$ , and we suppose  $\bar{t}=\text{const.}$  on the maximally-sliced hypersurface.

The original Schwarzschild time coordinate,  $t$ , is now the function of  $t(\bar{t}, r)$ , with

$$\left. \frac{\partial t}{\partial \bar{t}} \right|_{r=\text{const.}} = \alpha \sqrt{A} \quad (\text{B3})$$

$$\left. \frac{\partial t}{\partial r} \right|_{\bar{t}=\text{const.}} = -\frac{\sqrt{A}T}{r^2} \frac{1}{1-2M/r} \quad (\text{B4})$$

where  $T$  is an arbitrary function of  $\bar{t}$ , while  $A$  is given

$$A = \left(1 - \frac{2M}{r} + \frac{T^2}{r^4}\right)^{-1}, \quad (\text{B5})$$

using both Hamiltonian and momentum constraints. (B4) can be integrated as

$$t = -\frac{T}{M} \int_{M/r}^{X(T)} \frac{1}{1-2x} \frac{1}{\sqrt{1-2x+T^2M^{-4}x^4}} dx, \quad (\text{B6})$$

where  $X(T)$  is required to a smaller real root of the quartic equation,

$$1 - 2x + T^2M^{-4}x^4 = 0, \quad (\text{B7})$$

in order to be consistent with (B3) under the boundary condition,

$$\text{the smoothness across the Einstein-Rosen bridge, } r = r_{\min}, \text{ at } t = 0, \quad (\text{B8})$$

that turns  $\partial t / \partial r|_{r \rightarrow r_{\min}} \rightarrow \infty$  and  $T = T(r_{\min}) = \sqrt{r_{\min}^3(2M - r_{\min})}$ .

By identifying  $t \sim \bar{t}$  at spatial infinity, we get

$$\bar{t} = -\frac{T}{M} \int_0^{X(T)} \frac{1}{1-2x} \frac{1}{\sqrt{1-2x+T^2M^{-4}x^4}} dx, \quad (\text{B9})$$

where the integration across the pole at  $x = 1/2$  is taken in the sense of the principal value.

In summary, if we specified a parameter  $T$  ( $0 \leq T < 3\sqrt{3}/4$  corresponds to  $0 \leq \bar{t} < \infty$ ), then we obtain the coordinate time  $t$  and  $\bar{t}$  from (B6) and (B9) via (B7). Then we obtain the metric components by

$$\alpha(r, T) = \sqrt{1 - \frac{2M}{r} + \frac{T^2}{r^4}} \left[ 1 + \frac{dT}{d\bar{t}} \frac{1}{M} \int_0^{M/r} \frac{dx}{(1-2x+T^2M^{-4}x^4)^{2/3}} \right], \quad (\text{B10})$$

$$\beta(r, T) = \alpha A T r^{-2}, \quad (\text{B11})$$

and (B5), where  $dT/d\bar{t}$  in (B10) can be calculated using

$$\left( \frac{dT}{d\bar{t}} \right)^{-1} = \frac{d\bar{t}}{dT} = \lim_{Y \rightarrow X} \left[ \frac{T^2 M^{-5} X^4}{(1-2T^2 M^{-4} X^3)(2X-1)\sqrt{1-2Y+T^2 M^{-4} Y^4}} - \frac{1}{M} \int_0^Y \frac{dx}{(1-2x+T^2 M^{-4} x^4)^{3/2}} \right] \quad (\text{B12})$$

They are functions of  $r$  and the minimum value of  $r$  (that is, at a throat),  $r_{min}$ , is given by a larger real root of  $r^4 - 2Mr^3 + T^2 = 0$ . Note that the fact  $r_{min} \rightarrow (3/2)M$  when  $t \rightarrow \infty$  indicates the singularity avoidance property of maximal slicing condition. The comparison of this feature with the harmonic slicing condition is seen in [29].

- 
- [1] R. Arnowitt, S. Deser and C. W. Misner, “The Dynamics of General Relativity”, in *Gravitation: An Introduction to Current Research*, ed. by L. Witten, (Wiley, New York, 1962).
  - [2] J. W. York, Jr., “Kinematics and Dynamics of General Relativity”, in *Sources of Gravitational Radiation*, ed. by L. Smarr, (Cambridge, 1979) ; L. Smarr, J.W. York, Jr., Phys. Rev. D **17**, 2529 (1978).
  - [3] T. Nakamura and K. Oohara, in *Frontiers in Numerical Relativity* edited by C.R. Evans, L.S. Finn, and D.W. Hobill (Cambridge Univ. Press, Cambridge, England, 1989). M. Shibata and T. Nakamura, Phys. Rev. D **52**, 5428 (1995).
  - [4] T. W. Baumgarte and S. L. Shapiro, Phys. Rev. D **59**, 024007 (1999).
  - [5] M. Alcubierre, B. Brügmann, T. Dramlitsch, J. A. Font, P. Papadopoulos, E. Seidel, N. Stergioulas, and R. Takahashi, Phys. Rev. D **62**, 044034 (2000).
  - [6] Recent reviews are given by, *e.g.*, O. A. Reula, Living Rev. Relativ. **1998-3** at <http://www.livingreviews.org/>; H. Friedrich and A. Rendall, in *Einstein’s field equations and their physical interpretation*, ed. by B.G.Schmidt (Springer, Berlin 2000), available as gr-qc/0002074.  
See other references in [13]. As a latest one, we add: [10].
  - [7] C. Bona, J. Massó, E. Seidel and J. Stela, Phys. Rev. Lett. **75**, 600 (1995); Phys. Rev. D **56**, 3405 (1997).
  - [8] M. S. Iriondo and O.A. Reula, gr-qc/0102027.
  - [9] B. Kelly, P. Laguna, K. Lockitch, J. Pullin, E. Schnetter, D. Shoemaker, and M. Tiglio, Phys. Rev. D **64**, 084013 (2001).
  - [10] L. E. Kidder, M. A. Scheel and S. A. Teukolsky, Phys. Rev. D **64**, 064017 (2001).
  - [11] S. D. Hern, PhD thesis, gr-qc/0004036.
  - [12] S. Frittelli and O. A. Reula, Phys. Rev. Lett. **76**, 4667 (1996). See also J. M. Stewart, Class. Quantum Grav. **15**, 2865 (1998).
  - [13] H. Shinkai and G. Yoneda, Class. Quantum Grav. **17**, 4799 (2000).
  - [14] G. Yoneda and H. Shinkai, Phys. Rev. Lett. **82**, 263 (1999).
  - [15] G. Yoneda and H. Shinkai, Int. J. Mod. Phys. D **9**, 13 (2000).
  - [16] A. Ashtekar, Phys. Rev. Lett. **57**, 2244 (1986); Phys. Rev. D **36**, 1587 (1987); *Lectures on Non-Perturbative Canonical Gravity* (World Scientific, Singapore, 1991).
  - [17] G. Calabrese, J. Pullin, O. Sarbach and M. Tiglio, in preparation.
  - [18] A. Anderson and J. W. York, Jr, Phys. Rev. Lett. **82**, 4384 (1999).
  - [19] O. Brodbeck, S. Frittelli, P. Hübner and O.A. Reula, J. Math. Phys. **40**, 909 (1999).
  - [20] G. Yoneda and H. Shinkai, Class. Quantum Grav. **18**, 441 (2001).
  - [21] H. Shinkai and G. Yoneda, Phys. Rev. D **60**, 101502 (1999).
  - [22] F. Siebel and P. Hübner, Phys. Rev. D **64**, 024021 (2001).
  - [23] G. Yoneda and H. Shinkai, Phys. Rev. D **63**, 120419 (2001).
  - [24] S. Frittelli, Phys. Rev. D **55**, 5992 (1997).
  - [25] S. Detweiler, Phys. Rev. D **35**, 1095 (1987).
  - [26] D. Bernstein, D. W. Hobill, and L. L. Smarr, in *Frontiers in Numerical Relativity*, edited by C.R. Evans, L.S. Finn, and D.W. Hobill (Cambridge Univ. Press, 1989).
  - [27] K. Martel and E. Poisson, gr-qc/0001069 (2000).
  - [28] F. Estabrook, H. Wahlquist, S. Christensen, B. DeWitt, L. Smarr, and E. Tsiang, Phys. Rev. D. **7**, 2814 (1973).
  - [29] A. Geyer and H. Herold, Phys. Rev. D. **52**, 6182 (1995), Gen. Rel. Grav. **29**, 1257 (1997).
  - [30] H. Shinkai, G. Yoneda, and T. Ebisuzaki, in preparation.
  - [31] [17] reports that there is an apparent difference on numerical stability between these hyperbolicity levels, based on Kidder-Scheel-Teukolsky’s reformulation [10] of Anderson-York [18] and Frittelli-Reula [12] formulations.

No.	name	adjustments (non-zero part)	TRS	1st?	motivations
0	standard ADM	no adjustments	–	yes	
1	original ADM	$R_{ij} = \kappa_F \alpha \gamma_{ij}$	yes	yes	$\kappa_F = -1/4$ makes original ADM
2-a	Detweiler	(2.18)-(2.21), $\kappa_L$	no	no	proposed by Detweiler [25]
2-P	Detweiler P-part	$P_{ij} = -\kappa_L \alpha^3 \gamma_{ij}$	no	no	only use $P_{ij}$ term of Detweiler-type
2-S	Detweiler S-part	$S^k_{ij} = \kappa_L \alpha^2 [3(\partial_i \alpha) \delta_j^k - (\partial_l \alpha) \gamma_{ij} \gamma^{kl}]$	no	yes	only use $S^k_{ij}$ term of Detweiler-type
2-s	Detweiler s-part	$s^{kl}_{ij} = \kappa_L \alpha^3 [\delta_i^k \delta_j^l - (1/3) \gamma_{ij} \gamma^{kl}]$	no	no	only use $s^{kl}_{ij}$ term of Detweiler-type
3	simplified Detweiler	$P_{ij} = -\kappa_L \alpha \gamma_{ij}$	no	no	similar to above No.2-P, but $\alpha$ monotonic
4	constant $R_{rr}$	$R_{rr} = -\kappa_\mu \alpha$	no	yes	used by Penn State group [9]

TABLE I: List of adjustments we tested and plotted. (See more cases in Table.III). The column of adjustments are nonzero multipliers in terms of (2.13) and (2.14). The column ‘TRS’ means whether each adjusting term satisfy the time reversal symmetry or not based on the standard Schwarzschild coordinate. (‘No’ is the candidate that makes asymmetric amplification factors (AFs).) The column ‘1st?’ is for whether each adjusting term breaks the first-order feature of the standard constraint propagation equation, (2.11) and (2.12). (‘Yes’ keeps the system first-order, ‘No’ is the candidate of breaking hyperbolicity of constraint propagation.)

adjustment \ coordinate		standard (4.1)		isotropic (4.2)	iEF (4.3)	PG (4.4)
		exact	maximal	exact	$t_{iEF} = 0$	$t_{PG} = 0$
0	standard ADM	Fig.1(a)	Fig.8(a)	Fig.4(a)	Fig.4(b)	Fig.4(c)
1	original ADM	Fig.1(b)	Fig.8(b)			
2-a	Detweiler	Fig.2	Fig.8(c)	Fig.5(a)	Fig.5(b)	Fig.5(c)
2-P	Detweiler P-part	Fig.3(a)				
2-S	Detweiler S-part	Fig.3(b)				
2-s	Detweiler s-part	Fig.3(c)				
3	simplified Detweiler	Fig.3(d)		Fig.6(a)	Fig.6(b)	Fig.6(c)
4	constant $R_{rr}$				Fig.7(a)	Fig.7(b)

TABLE II: List of figures we present in this article. The adjustments are explained in Table. I.

No.	No. in Table.I	adjustment	1st?	Sch/iso coords.			iEF/PG coords.	
				TRS	real.	imag.	real.	imag.
0	0	– no adjustments	yes	–	–	–	–	–
P-1	2-P	$P_{ij} - \kappa_L \alpha^3 \gamma_{ij}$	no	no	makes 2 Neg.	not apparent	makes 2 Neg.	not apparent
P-2	3	$P_{ij} - \kappa_L \alpha \gamma_{ij}$	no	no	makes 2 Neg.	not apparent	makes 2 Neg.	not apparent
P-3	-	$P_{ij} \quad P_{rr} = -\kappa$ or $P_{rr} = -\kappa \alpha$	no	no	slightly enl.Neg.	not apparent	slightly enl.Neg.	not apparent
P-4	-	$P_{ij} - \kappa \gamma_{ij}$	no	no	makes 2 Neg.	not apparent	makes 2 Neg.	not apparent
P-5	-	$P_{ij} - \kappa \gamma_{rr}$	no	no	red. Pos./enl.Neg.	not apparent	red.Pos./enl.Neg.	not apparent
Q-1	-	$Q^k_{ij} \quad \kappa \alpha \beta^k \gamma_{ij}$	no	no	N/A	N/A	$\kappa \sim 1.35$ min. vals.	not apparent
Q-2	-	$Q^k_{ij} \quad Q^r_{rr} = \kappa$	no	yes	red. abs vals.	not apparent	red. abs vals.	not apparent
Q-3	-	$Q^k_{ij} \quad Q^r_{ij} = \kappa \gamma_{ij}$ or $Q^r_{ij} = \kappa \alpha \gamma_{ij}$	no	yes	red. abs vals.	not apparent	enl.Neg.	enl. vals.
Q-4	-	$Q^k_{ij} \quad Q^r_{rr} = \kappa \gamma_{rr}$	no	yes	red. abs vals.	not apparent	red. abs vals.	not apparent
R-1	1	$R_{ij} \quad \kappa_F \alpha \gamma_{ij}$	yes	yes	$\kappa_F = -1/4$ min. abs vals.		$\kappa_F = -1/4$ min. vals.	
R-2	4	$R_{ij} \quad R_{rr} = -\kappa_\mu \alpha$ or $R_{rr} = -\kappa_\mu$	yes	no	not apparent	not apparent	red.Pos./enl.Neg.	enl. vals.
R-3	-	$R_{ij} \quad R_{rr} = -\kappa \gamma_{rr}$	yes	no	enl. vals.	not apparent	red.Pos./enl.Neg.	enl. vals.
S-1	2-S	$S^k_{ij} \quad \kappa_L \alpha^2 [3(\partial_{(i} \alpha) \delta_{j)}^k - (\partial_l \alpha) \gamma_{ij} \gamma^{kl}]$	yes	no	not apparent	not apparent	not apparent	not apparent
S-2	-	$S^k_{ij} \quad \kappa \alpha \gamma^{lk} (\partial_l \gamma_{ij})$	yes	no	makes 2 Neg.	not apparent	makes 2 Neg.	not apparent
p-1	-	$p^k_{ij} \quad p^r_{ij} = -\kappa \alpha \gamma_{ij}$	no	no	red. Pos.	red. vals.	red. Pos.	enl. vals.
p-2	-	$p^k_{ij} \quad p^r_{rr} = \kappa \alpha$	no	no	red. Pos.	red. vals.	red.Pos/enl.Neg.	enl. vals.
p-3	-	$p^k_{ij} \quad p^r_{rr} = \kappa \alpha \gamma_{rr}$	no	no	makes 2 Neg.	enl. vals.	red. Pos. vals.	red. vals.
q-1	-	$q^{kl}_{ij} \quad q^{rr}_{ij} = \kappa \alpha \gamma_{ij}$	no	no	$\kappa = 1/2$ min. vals.	red. vals.	not apparent	enl. vals.
q-2	-	$q^{kl}_{ij} \quad q^{rr}_{rr} = -\kappa \alpha \gamma_{rr}$	no	yes	red. abs vals.	not apparent	not apparent	not apparent
r-1	-	$r^k_{ij} \quad r^r_{ij} = \kappa \alpha \gamma_{ij}$	no	yes	not apparent	not apparent	not apparent	enl. vals.
r-2	-	$r^k_{ij} \quad r^r_{rr} = -\kappa \alpha$	no	yes	red. abs vals.	enl. vals.	red. abs vals.	enl. vals.
r-3	-	$r^k_{ij} \quad r^r_{rr} = -\kappa \alpha \gamma_{rr}$	no	yes	red. abs vals.	enl. vals.	red. abs vals.	enl. vals.
s-1	2-s	$s^{kl}_{ij} \quad \kappa_L \alpha^3 [\delta_{(i}^k \delta_{j)}^l - (1/3) \gamma_{ij} \gamma^{kl}]$	no	no	makes 4 Neg.	not apparent	makes 4 Neg.	not apparent
s-2	-	$s^{kl}_{ij} \quad s^{rr}_{ij} = -\kappa \alpha \gamma_{ij}$	no	no	makes 2 Neg.	red. vals.	makes 2 Neg.	red. vals.
s-3	-	$s^{kl}_{ij} \quad s^{rr}_{rr} = -\kappa \alpha \gamma_{rr}$	no	no	makes 2 Neg.	red. vals.	makes 2 Neg.	red. vals.

TABLE III: List of adjustments we tested in the Schwarzschild spacetime. The column of adjustments are nonzero multipliers in terms of (2.13) and (2.14). The column ‘1st?’ and ‘TRS’ are the same with Table. I. The effects to amplification factors (when  $\kappa > 0$ ) are commented for each coordinate system and for real/imaginary parts of AFs, respectively. The ‘N/A’ means that there is no effects due to the coordinate properties; ‘not apparent’ means the adjustment does not change the AFs effectively according to our conjecture; ‘enl./red./min.’ means enlarge/reduce/minimize, and ‘Pos./Neg.’ means positive/negative, respectively. These judgements are made at the  $r \sim O(10M)$  region on their  $t = 0$  slice.

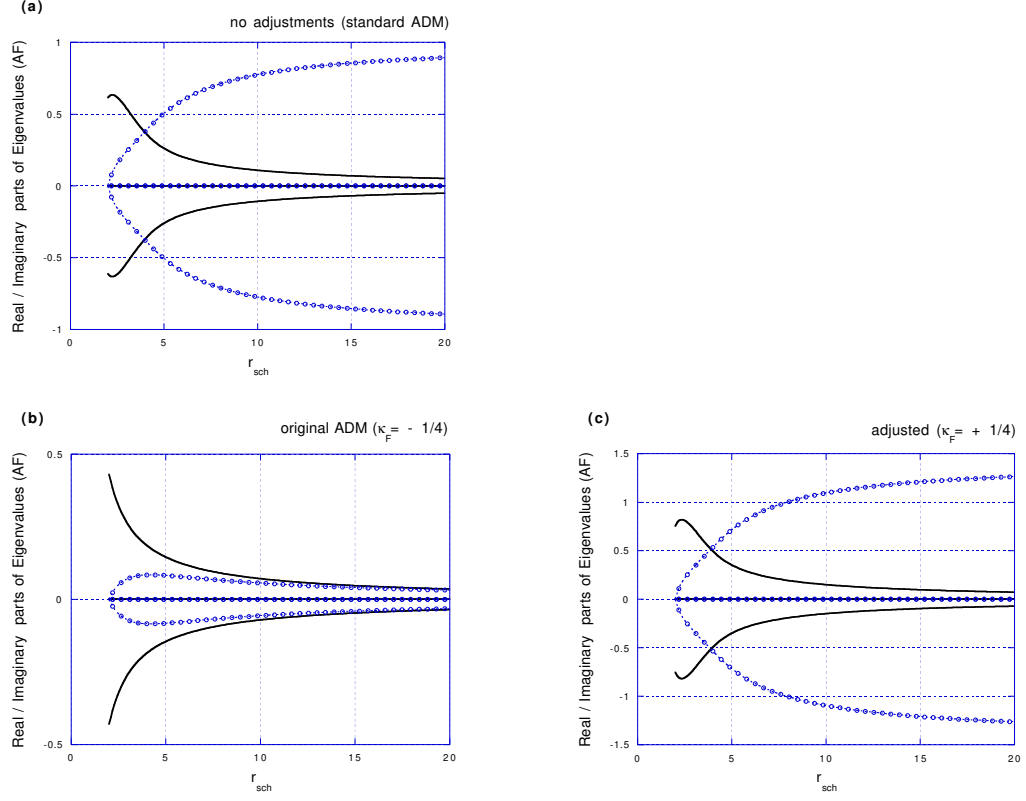


FIG. 1: Amplification factors (AFs, eigenvalues of homogenized constraint propagation equations) are shown for the standard Schwarzschild coordinate, with (a) no adjustments, i.e., standard ADM, (b) original ADM ( $\kappa_F = -1/4$ ) and (c) adjusted version with different signature,  $\kappa_F = +1/4$  [see eq. (2.17)]. The solid lines and the dotted lines with circles are real parts and imaginary parts, respectively. They are four lines each, but actually two eigenvalues are zero for all cases. Plotting range is  $2 < r \leq 20$  using Schwarzschild radial coordinate. We set  $k = 1$ ,  $l = 2$ , and  $m = 2$  throughout the article.



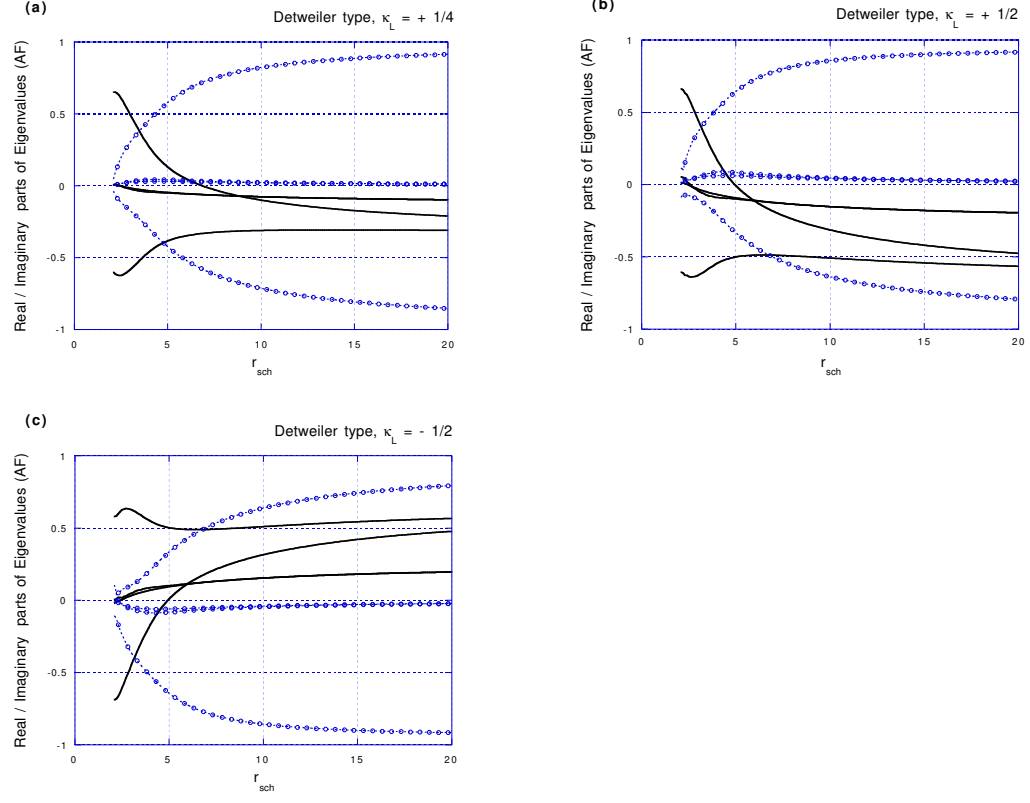


FIG. 2: Amplification factors of the standard Schwarzschild coordinate, with the Detweiler type adjustments, (2.18)-(2.21). Multipliers used in the plot are (a)  $\kappa_L = +1/4$ , (b)  $\kappa_L = +1/2$ , and (c)  $\kappa_L = -1/2$ . Plotting details are the same with Fig.1.

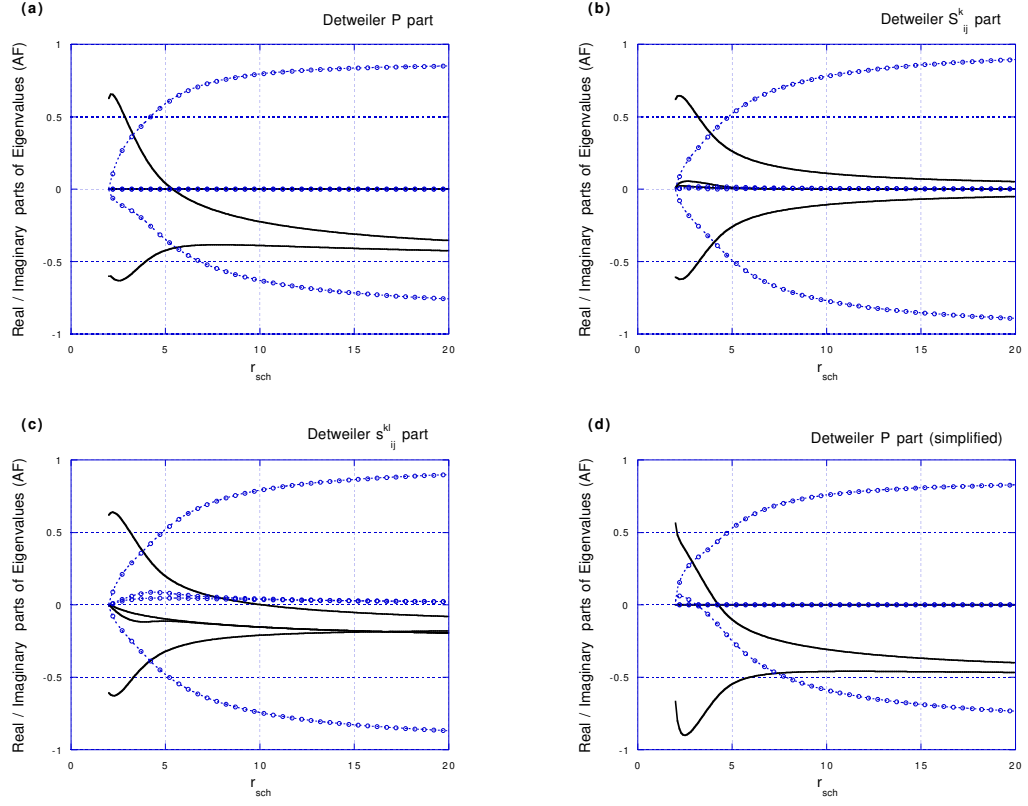


FIG. 3: Amplification factors of the standard Schwarzschild coordinate, with the Detweiler type (partial contributions) adjustments. Fig.(a) is the case No. 2-P in Table.I, adjusting with  $P_{ij} = -\kappa_L \alpha^3 \gamma_{ij}$ , i.e. (2.18), and else zero. Similarly, (b) is No. 2-S,  $S^k_{ij}$ -part (2.20) and else zero, and (c) is No. 2-s,  $s^{kl}_{ij}$ -part (2.21) and else zero. Fig. (d) is No. 3,  $P_{ij} = -\kappa_L \alpha \gamma_{ij}$  and else zero, which is a minor modification from (a). We used  $\kappa_L = +1/2$  for all plots. Plotting details are the same with Fig.1.

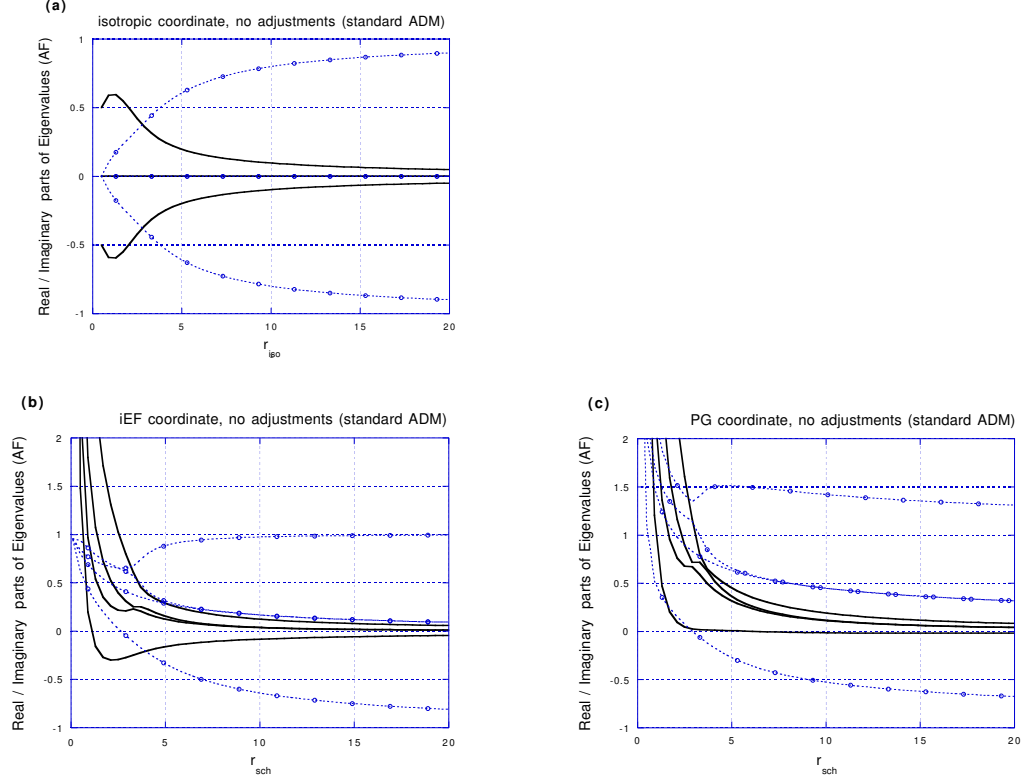


FIG. 4: Comparison of amplification factors between different coordinate expressions for the standard ADM formulation (i.e. no adjustments). Fig. (a) is for the isotropic coordinate (4.2), and the plotting range is  $1/2 \leq r_{iso}$ . Fig. (b) and (c) are for the iEF coordinate (4.3) and for the PG coordinate (4.4), respectively, and we plot lines on the  $t = 0$  slice for each expression. [See Fig.1(a) for the standard Schwarzschild coordinate.] The solid four lines and the dotted four lines with circles are real parts and imaginary parts, respectively.

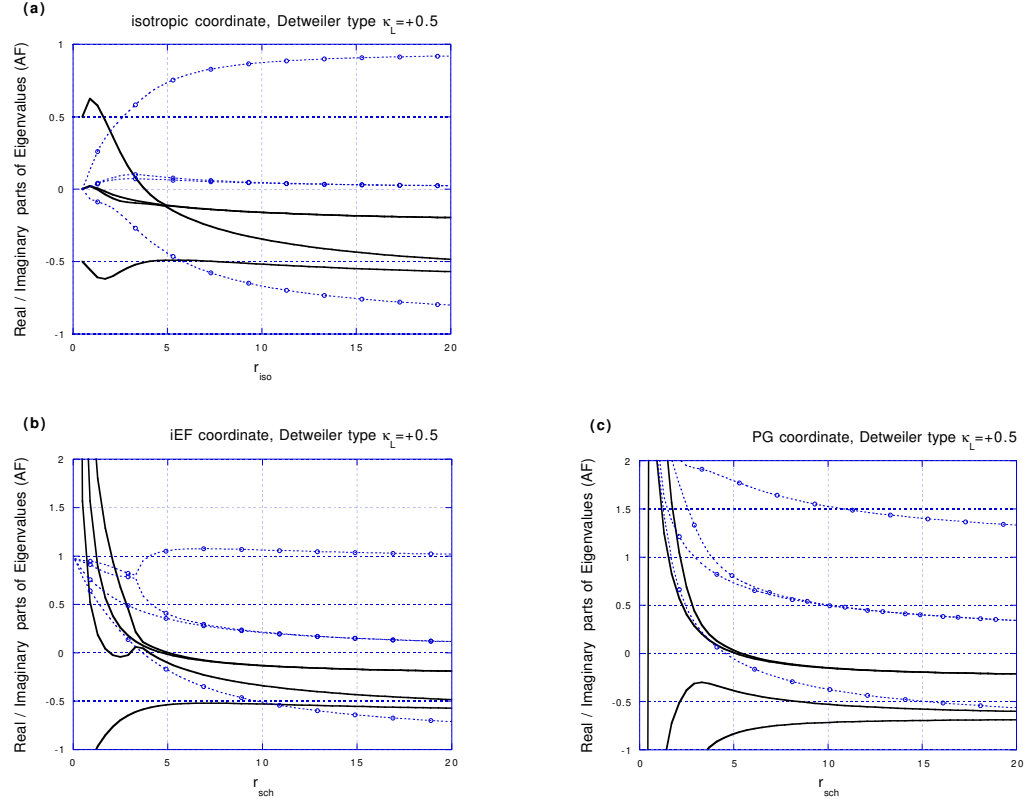


FIG. 5: Similar comparison with Fig.4, but for Detweiler adjustments.  $\kappa_L = +1/2$  for all plots. [See Fig.2(b) for the standard Schwarzschild coordinate.]

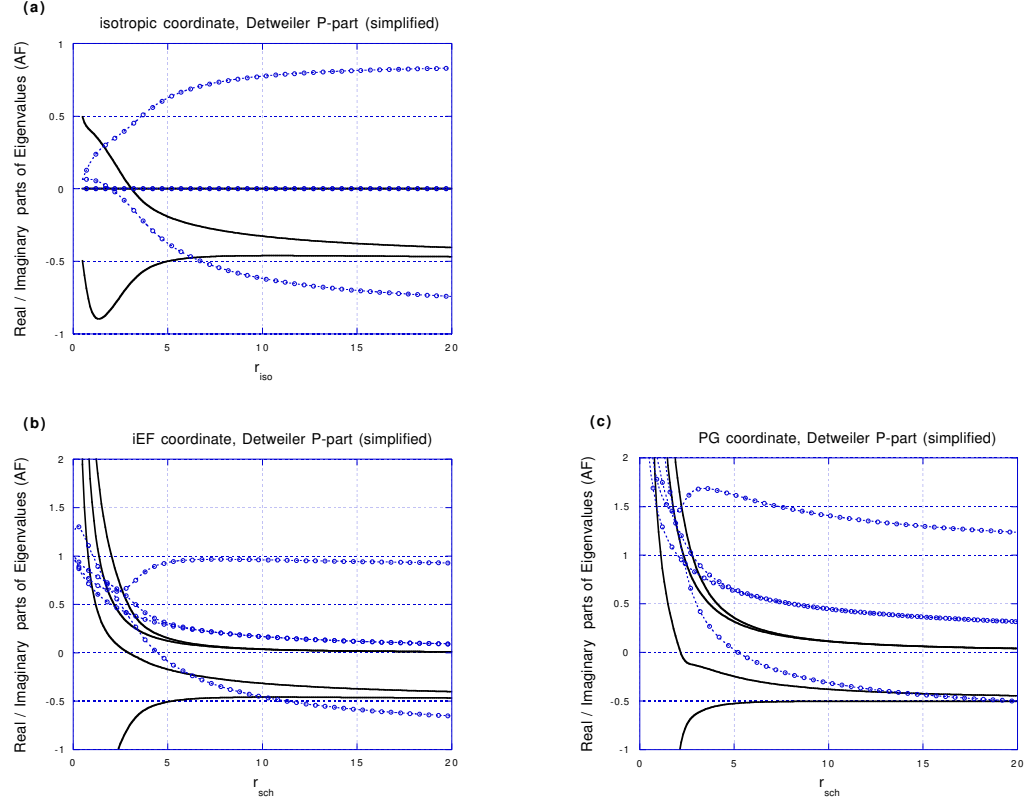


FIG. 6: Similar comparison with Fig.4, but for simplified Detweiler adjustments (No.3 in Table. I).  $\kappa_L = +1/2$  for all plots. [See Fig.3(d) for the standard Schwarzschild coordinate.]

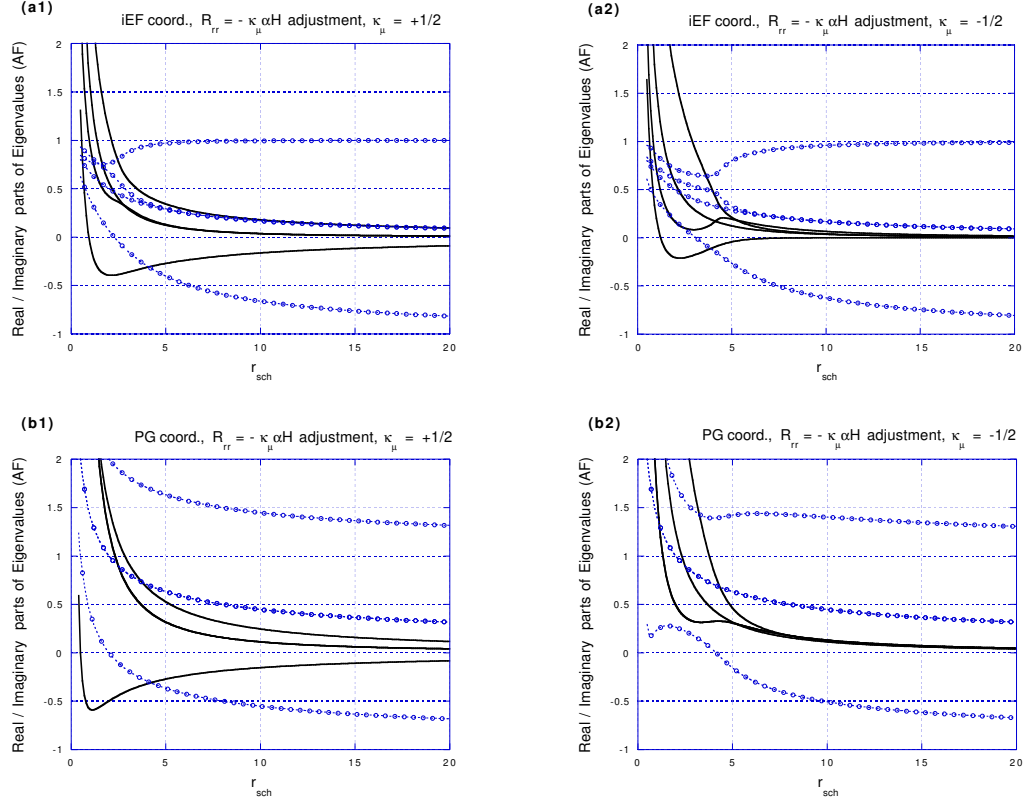


FIG. 7: Amplification factors of the adjustment No.4 in Table. I.  $\kappa_{\mu} = +1/2, -1/2$  for iEF/PG coordinates. [See Fig.4(b)(c) for the standard ADM system.]

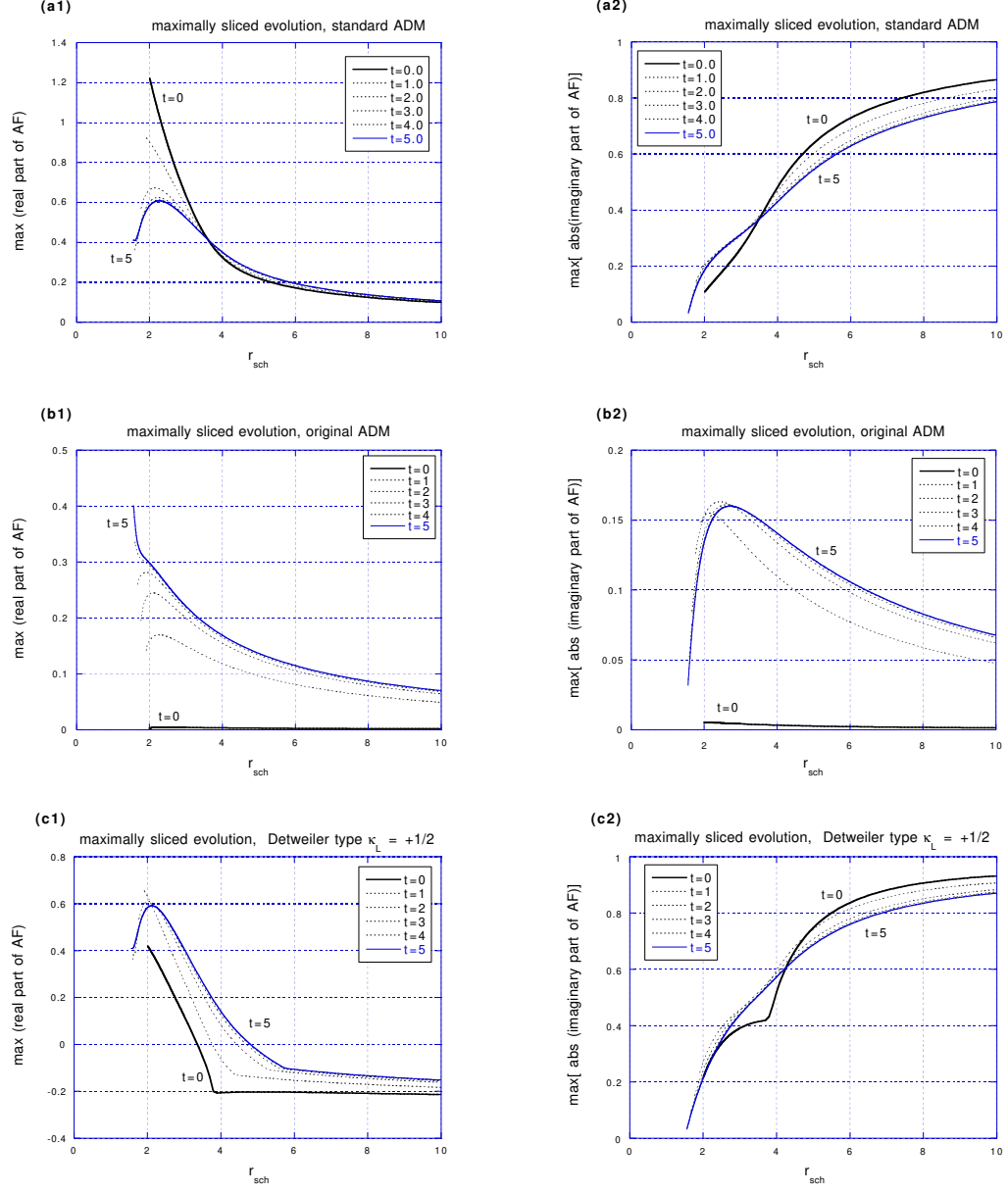


FIG. 8: Amplification factors of snapshots of maximally-sliced evolving Schwarzschild spacetime. Fig (a1) and (a2) are of the standard ADM formulation (real and imaginary parts, respectively), (b1) and (b2) are the original ADM formulation, (c1) and (c2) are Detweiler's adjustment ( $\kappa_L = +1/2$ ). Lines in (a1), (b1) and (c1) are the largest (positive) AF on each time slice, while lines in (a2), (b2) and (c2) are the maximum imaginary part of AF on each time slice. The time label  $t$  in plots is  $\bar{t}$  in the Appendix B. The lines start at  $r_{min} = 2$  ( $\bar{t} = 0$ ) and  $r_{min} = 1.55$  ( $\bar{t} = 5$ ).